Theor Chem Acc (2006) 115: 32–36
DOI 10.1007/s00214-005-0669-5

REGULAR ARTICLE

Y. Ouyang · H. Chen · X. Zhong

Ab initio studies of small Al_mFe_n clusters

Received: 23 March 2005 / Accepted: 24 March 2005 / Published online: 4 November 2005

Abstract The equilibrium geometrical structures of small Al_mFe_n clusters have been determined through *ab initio* calculation of the cluster total energy at the UB3LYP/Lanl2dz level. For dimers of iron and aluminum, the dissociation energies, the equilibrium atomic distances, and the vibrational frequencies were calculated. The agreement between calculations and experiments is reasonable. The ground stable geometrical structures of Fe_4, $FeAl_3$, Fe_3Al and Fe_2Al_2 clusters favor three-dimension configurations, but Al_4 tetramers are planar structures. The Al-rich tetramers are more stable than the other two composition tetramers. This is different from that of bulk alloys.

Keywords Ab initio · Cluster · Iron · Aluminum

1 Introduction

In a cluster research, the fundamental problem is the determination of the geometrical structures assumed by the clusters, which may affect their optical, magnetic and chemical properties, thermal stability and dynamical behavior. Theoretical investigations of micro clusters by *ab initio* quantum mechanical calculations have attracted great attention. More studies focus on pure clusters. For iron clusters, Noro et al. [1] obtained the ground state of the dimer with multireference self-consistent-field (MCSCF) and multireference configuration interaction (CI) calculations. They concluded that the combination of the *d* electrons to the bonding is important. Bollone et al. [2] have studied the structure and spin of cluster up to seven atoms with Car-Parrinello molecular dynamic simulations. The trend is similar to that predicted with empirical pair-potentials. Chen et al. [3] investigated the magnetic and structural ordering in iron clusters Fe_n with a first-principle all electron linear-combination of Gaussian orbital method. The ground states are all ferromagnetic with the highest dimensional geometry. Dieguez et al. [4] simulated the ground state configurations of Fe_n with semiempirical methods of embedded atom method (EAM) [5]. For clusters of aluminum, a great deal of theoretical calculations has been performed [6,7]. The cluster size reaches several hundreds atoms. Some works on binary FeAl clusters have been published [4,8–10].

Iron aluminides are an important class of intermetallic compounds with high oxidation and corrosion resistance, low density and interesting magnetic properties. From the phase diagram, the bulk alloys form ordered Fe_3Al, FeAl and $FeAl_3$ compounds. The results of experiment [11] on FeAl nanoparticles indicate that they are magnetic. This is different from that of ordered compounds. The ferromagnetic behaviors arose from the clustering of iron atoms. For micro Al_mFe_n clusters, the structures and mixing can be very different from that in bulk. The partial segregation could lead to clustering of iron sites. Dieguez et al. [4] studied the Fe-rich cluster using molecular dynamics simulations based on EAM. Reddy et al. [9] obtained the structures and magnetic properties of Fe-rich Fe-Al binary cluster. The geometric arrangement of $(FeAl)_n$ are different from the bulk ordering and dominated by the Fe-Fe clustering. Are the lowest-lying states the structures of clustering of iron atom? How does the composition affect the structural stability of binary cluster? The density functional theory (DFT) has been used to study the geometric stability of binary Al_mFe_n cluster.

2 Computational details

The DFT method with B3LYP [12,13] exchange-correlation potential and an effective core potential LanL2DZ basis sets [14–16] are used in the present calculations. The exchange term of B3LYP consists of hybrid Hartree-Fock and local spin density (LSD) exchange functions with Beck's gradient correlation to LSD exchange [17]. The correlation term of unrestricted B3LYP consists of the VWN3 local correlation functional and Lee, Yang and Parr (LYP) correlation correction functional. The UB3LYP predictions are in qualitative

---

Y. Ouyang (✉)· H. Chen · X. Zhong
Department of Physics, Guangxi University,
Nanning 530004, P R China
E-mail: ouyangyf@gxu.edu.ch

Table 1 The bond length, binding energy and vibrational frequency of dimers

Molecule		R_e(Å)	$-E_b$(eV/atom)	ω(cm^{-1})	state	Refs.
Fe_2	$D_{\infty h}$	2.26	3.75	305.5	Multiplicity = 9	Present
		2.02,1.87	0.65	299.6		[20–23]
		1.98	2.02	418	Ferromagnetic	[3]
		2.20	0.97	209	Antiferromagnetic	[3]
		1.83	0.85	461	Paramagnetic	[3]
		2.10	1.73	390		[24]
		2.01	2.0	402		[25]
		2.40		204		[26]
		2.06	0.79	260.9		[1]
		1.96	1.45		$^7\Delta_u$	[27]
		2.02	1.88			[9]
		2.13	1.48			[9]
		1.88	0.82		S=0	[2]
		2.06	1.78		S=4	[2]
Al_2	$D_{\infty h}$	2.59	0.49	289.4	Multiplicity=3	Present
		2.47	0.75	350.0		[28]
		2.23	0.58	647.0		[6]
		2.709	0.68	284.0	Multiplicity=3	[7]
		2.49	0.92		S=3	[9]
		2.48	0.82		S=3	[9]
FeAl	$C_{\infty v}$	2.50	2.64	280.1	Multiplicity=2	Present
		2.43	1.65			[9]
		2.41	1.01			[9]

agreement with experimental values. In general, the DFT method overestimates the energies, and it gives shorter bond length than the experimental results. However, the optimizied structures predicted at the UB3LYP level are in good agreement with the results of experiment. LanL2DZ basis sets are getting to be widely used to calculate the equilibrium geometries and spectroscopic properties of clusters, particularly in the investigation on clusters with heavy atoms [17]. The standard LanL2DZ basis sets of ECP theory are capable of generating results of very satisfactory quality for transition metal compounds [18]. The examination of equilibrium bond lengths and angles reveals deviations of typically 1–6%. The calculated ionization energy of iron and aluminum are 7.48 eV and 6.20 eV, respectively, while the experimental values are 7.92 eV and 5.99 eV respectively.

All density functional theory (DFT) computations are performed with Gaussian 98 [19] program package. Geometries are optimized at the hybrid functional DFT-UB3LYP level, employing LanL2DZ basis sets.

The binding energy per atom of clusters is defined as

$$E_b = \frac{\left[E_{\text{cluster}} - mE_{\text{Fe}}^{\text{at}} - nE_{Al}^{\text{at}}\right]}{m+n} \tag{1}$$

where E_{cluster} is energy of alloy cluster, $E_{\text{Fe}}^{\text{at}}$ is pure iron atom and $E_{\text{Al}}^{\text{at}}$ is pure aluminum atom.

3 Results and discussions

3.1 Dimer

The calculated binding energies, equilibrium geometries and vibrational frequencies of dimers are given in Table 1. The experimental results and the results obtained by other research workers are also included for comparison. From Table 1, it can be seen that the present results for equilibrium bond length, binding energy, and vibrational frequency of iron dimer are larger than those of experiments [20–23]. The present bond length is close to that of Chen et al. [3] obtained for antiferromagnetic state of iron dimer and that of Reddy et al [9]. The available theoretical binding energies [1–3, 9, 24, 25, 27] range from −0.785 to −2.025 eV/atom, where experimental binding energy is −0.65 eV/atom. The present result is −3.75 eV/atom. The vibrational frequency is more closer to that of experiment [23] than those obtained by other theoretical studies [1, 3, 24–27].

The calculated bond length, binding energy and vibrational frequency of Al dimer are 2.59 angstrom, −0.49 eV/atom and 289 cm^{-1} respectively, where corresponding experimental values are 2.47 Å, −0.75 eV/atom and 350 cm^{-1} respectively [28]. The bond length is longer than that of experiment and those obtained by other theoretical calculations [6, 9]. The binding energy is less than those of experiment and theories. But, the vibrational frequency is closer to experimental values [28]. Schultz et al. [7] calculated the bond length and binding energy using several multilevel methods. Results of the present calculations are coincide with those they recommended.

The investigations of binary dimer are limited. Reddy et al. [9] calculated the bond length and binding energy. Their results are smaller than those obtained in the present results.

3.2 Trimer

The present calculations show that for Fe_3 and Al_3 trimers, there are two possible stable structures: the linear and

Table 2 Geometries, binding energy and multiplicity *S* of trimers

geometry		1-2-3	R_{12}(Å)	R_{23}(Å)	R_{13}(Å)	$-E_b$(eV/atom)	S	Refs.
	$D_{\infty h}$	Fe-Fe-Fe	2.37	2.37	4.74	3.835	5	Present
			1.92	1.92	3.84	1.789		[3]
			1.87	1.87	3.74	1.529		[3]
			2.12	2.07	4.19	1.175		[2]
		Al-Al-Al	2.66	2.66	5.32	0.849	4	Present
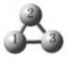	D_{3h}	Fe-Fe-Fe	2.10	2.10	2.10	5.078	1	Present
			2.04	2.04	2.04	2.602		[3]
			2.10	2.10	2.10	1.41		[29]
		Al-Al-Al	2.63	2.63	2.63	0.877	2	Present
			2.52	2.52	2.52	1.363	2	[7]
			2.26	2.26	2.26	2.237		[30]
	$D_{\infty h}$	Fe-Al-Fe	2.43	2.43	4.86	3.168	6	Present
		Al-Fe-Al	2.49	2.49	4.98	2.009	5	Present
	$C_{\infty v}$	Fe-Fe-Al	2.46	2.50	4.96	3.256	8	Present
		Al-Al-Fe	2.42	2.77	5.19	2.065	5	Present
	C_{2v}	Fe-Al-Fe	2.66	2.66	2.65	3.499	8	Present
		Al-Fe-Al	2.55	2.55	2.65	2.275	3	Present

triangular structures in each case. The bond length of iron trimer with linear structure is longer than those obtained by Chen et al. [3] and Ballone et al. [2]. The binding energy is larger than those obtained by Chen et al. and Ballone et al. As for the triangular structure, the bond length is larger than that of Chen et al. but coincide with that of Castro et al. [29]. The binding energy is greater than that of Castro and that of Chen et al.

As for the Al_3 trimer with triangular structure, the bond length obtained in the present calculation is longer than those of Majumder et al. [30] and Schultz et al. [7], while the binding energy is smaller. The equilateral triangular structures of trimer of iron or aluminum are found to be the most stable geometrical structures.

There are three possible isomer structures for Fe_2Al and $FeAl_2$ trimers, the symmetric and asymmetric linear structures and the triangular structures in each case. The triangular structures are found to be the most stable geometrical structures. For Fe_2Al, the bond angle is 59.8 degrees and in $FeAl_2$ the angle is 62.6 degrees.

For the linear forms of 3-atom binary clusters, the present calculation reveals that the asymmetrical chain of Fe-Fe-Al is more stable than the symmetrical chain of Fe-Al-Fe for Fe_2Al. Al-Al-Fe trimer is more stable than the trimer of Al-Fe-Al. Table 2 lists our results for the possible stable equilibrium geometries and binding energies for trimers and other available results.

3.3 Tetramers

For monatomic tetramers, the bond lengths and binding energies of Fe_4 and Al_4 are given in Table 3. The ground state structure of Fe_4 is a butterfly shaped structure. Chen et al. [3] found that Fe_4 is tetrahedral structure. However, Ballone et al. [2] found that the ground state of Fe_4 is a butterfly (C_{2V}) structure. The bond lengths of the present calculation are longer than those obtained by Chen et al. and Ballone et al.

There have been several calculations of the aluminum tetramer [7,30–35]. A tetrahedral structure is favored by Majumder et al. [30], Ueno et al. [31], Jones [32] and Meier et al. [33], but Schultz et al. [7], Pacchioni et al. [34] and Petterson et al. [35] predicted a rhombic ground state.

The present calculations have found numerous local minima in the energy surface of Al_4. The most stable structure is a planar rhombus, but the square is very close in energy (0.054 eV higher). This is in good agreement with those of Pacchioni et al. [34] and Meier et al. [33] (0.005 eV and 0.04 eV higher, respectively).

There is a larger number of possible isomers for binary clusters in contrast to monatomic clusters. As expected, the number of stable isomers increases rapidly with cluster size and atomic composition. There are several possible stable structures for Fe_3Al and $FeAl_3$ tetramers. The bond length and binding energies are also included in Table 3. The ground

Table 3 Geometries, binding energies and multiplicity *S* of tetramers (the bond length in Angstrom, binding energy in eV/atom

geometry	Sym.	1-2-3-4	R_{12}	R_{23}	R_{34}	R_{13}	R_{24}	R_{14}	$-E_b$	S	Refs.
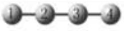	$D_{\infty h}$	Al-Al-Al-Al	2.45	2.53	2.45				0.549	7	Present
	$D_{\infty h}$	Fe-Fe-Fe-Fe	2.37	1.97	2.37				3.695	5	Present
			1.92	1.92	1.92				1.380		[3]
	D_{4h}	Al-Al-Al-Al	2.75	2.75	2.75	3.89	3.89	2.75	1.115	3	Present
	C_{2V}	Fe-Fe-Fe-Fe	2.24	2.34	2.24	3.24	3.24		3.164	9	Present
	D_{4h}		1.96	1.96	1.96	2.77	2.77		2.525		[3]
	D_{4h}		2.21	2.21	2.21	3.12	3.12		2.81		[2]
	D_{2h}	Al-Al-Al-Al	2.67	2.67	2.67	3.23	4.26	2.67	1.061	3	Present
			2.57	2.57	2.57	2.92	4.24	2.57	1.488		[7]
	D_{2h}	Fe-Fe-Fe-Fe	2.62	2.62	2.62	2.42	4.64	2.62	4.145	3	Present
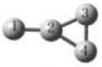	C_{2v}	Al-Al-Al-Al	2.81	2.67	2.52	5.31	2.67	5.31	1.018	1	Present
	C_{2v}	Fe-Fe-Fe-Fe	2.46	2.61	2.06	4.96	2.61	4.96	4.302	7	Present
	C_{2v}	Al-Al-Al-Al	2.61	2.88	4.11	2.88	2.88	2.88	0.979	3	Present
	T_h		2.33	2.33	2.33	2.33	2.33	2.33	2.778		[27]
	C_{2v}	Fe-Fe-Fe-Fe	2.64	2.53	2.64	2.64	2.64	2.69	4.557	3	Present
	T_h		2.12	2.12	2.12	2.12	2.12	2.12	2.282		[3]
	T_h		2.25	2.25	2.25	2.25	2.25	2.25	3.073		[3]
	T_h		2.17	2.17	2.17	2.17	2.43	2.17	3.55		[2]
	$C_{\infty v}$	Fe-Fe-Fe-Al	2.41	2.52	2.31				3.455	6	Present
	$C_{\infty v}$	Al-Al-Al-Fe	2.69	2.52	2.40				1.881	6	Present
	$C_{\infty v}$	Fe-Fe-Al-Fe	2.36	2.57	2.30				3.461	6	Present
	$C_{\infty v}$	Al-Al-Fe-Al	2.58	2.51	2.49				1.786	6	Present
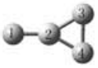	C_{2v}	Fe-Al-Fe-Fe	2.40	2.44	2.26	4.71	2.44	4.71	3.569	10	Present
		Al-Fe-Al-Al	2.45	2.49	2.80	4.72	2.49	4.72	1.954	4	
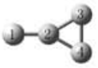	C_{2v}	Al-Fe-Fe-Fe	2.67	2.51	4.33	258	2.51	2.58	3.618	4	Present
		Fe-Al-Al-Al	2.42	2.78	2.67	5.04	2.78	5.04	1.944	6	
	C_{2v}	Al-Fe-Fe-Fe	2.52	2.59	2.59	4.53	2.36	2.52	3.603	2	Present
		Fe-Al-Al-Al	2.52	2.93	2.93	4.71	2.76	2.52	2.018	2	
	C_{2v}	Al-Fe-Fe-Fe	2.67	2.29	2.47	2.67	2.47	2.68	3.755	8	Present
	C_{3v}	Fe-Al-Al-Al	2.39	3.19	3.19	2.39	3.19	2.39	2.559	4	
	$C_{\infty v}$	Fe-Al-Fe-Al	2.42	2.44	2.51				2.690	5	Present
	$D_{\infty h}$	Al-Fe-Fe-Al	2.39	2.31	2.39				2.539	5	Present
	$D_{\infty h}$	Fe-Al-Al-Fe	2.37	2.43	2.37				2.676	9	Present
	$C_{\infty v}$	Fe-Fe-Al-Al	2.46	2.45	2.97				2.697	7	Present
	C_{2v}	Fe-Fe-Al-Al	2.49	3.55	2.67	2.45	2.45	3.55	2.843	5	Present
	D_{2h}	Fe-Al-Fe-Al	2.48	2.48	2.48	4.14	2.74	2.48	2.851	7	Present
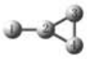	C_{2v}	Fe-Fe-Al-Al	2.50	2.55	2.72	4.85	2.55	4.85	2.810	3	Present
		Al-Al-Fe-Fe	2.77	2.46	3.88	4.70	2.46	4.70	2.761	7	
	D_{2h}	Al-Fe-Al-Fe	2.79	2.79	2.58	2.78	2.52	2.58	3.075	3	Present

state structure of Fe_3Al is an asymmetric pyramid and $FeAl_3$ tetramer has also a three-dimensional structure, which is a symmetric triangular pyramid. For the Fe_3Al Y-planar structure, the segregated configuration is more stable than that of the mixed one. However, for $FeAl_3$ Y-planar structure, the mixed configuration is more stable than that of segregated one. This indicates that the Fe–Fe clustering leads to low energy structure.

Reddy et al. [9] predicted the stable structures of $(FeAl)_n$ clusters. They found that the ground state of $(FeAl)_2$ tetramer is a distorted tetrahedral structure. The total energy of planar structure (rhombic) is only just above the ground state 0.7 eV.

The present calculations for $(FeAl)_2$ tetramers predicted a ground state with distorted tetrahedral structure. The Y-planar structure is close in energy to the ground state (0.224 eV higher).

How does the binding energy of ground state of tetramers depend on composition? To show this the energy difference of binary cluster relative to the monatomic cluster is defined as that of bulk alloys, namely,

$$\Delta E = E_b^{\text{binary}} - \frac{nE_b^{\text{Fe}} + mE_b^{\text{Al}}}{m+n} \tag{2}$$

The calculated energy differences indicate that the Fe_3Al tetramer is the most stable, the next is $FeAl_3$ tetramer and the least stable is Fe_2Al_2, the energies being −0.072 eV/atom, −0.624 eV/atom and −0.394 eV/atom respectively. The formation energies of bulk Fe_3Al, $FeAl_3$ and FeAl intermetallic compounds are −0.32, −0.29, and −0.26 eV/atom respectively [36]. The energy dependence on the composition for tetramer clusters is different from that of bulk compounds.

4 Conclusions

The ground state structures and binding energies for Al_mFe_n small clusters have been obtained with DFT. The calculations indicate that for the ground state structures of aluminum monatomic is planar structure while the highest dimension structures are favored for the ground state iron monatomic clusters and binary clusters. The Fe–Fe clustering leads to low the binding energy of binary cluster. The dependence of binding energy on composition is different from that of bulk intermetallic compounds.

Acknowledgements Y F Ouyang and H M Chen would like to acknowledge Dr Y P Feng from National University of Singapore for valuable discussion and pre-reading the manuscript. This work has been supported by the National Natural Science Foundation of China (10264001 and 50261001).

References

1. Noro T, Ballard C, Palmer MH, Tatewaki H (1994) J Chem Phy 100:452
2. Ballone P, Jones RO (1995) Chem Phys Lett 233:632
3. Chen JL, Wang CS, Jackson KA, Pederson MR (1991) Phys Rev B44:573
4. Dieguez O, Longo RC, Rey C, Callego LJ (1999) Euro Phys J D7:573
5. Foiles SM, Baskes MI, Daw MS (1986) Phys Rev B33:7983
6. Quek HK, Feng YP, Ong CK (1997) Z Physik D42:309
7. Schultz NE, Staszewska G, Staszewski P, Truhlar DG (2004) J Phys Chem B108:4850
8. Reddy BV, Deevi SC, Lilly AC, Jena P (2001) J Phys Condens Matt 13:8363
9. Reddy BV, Khanna SN, Deevi SC (2001) Chem Phys Lett 333:465
10. Li H, Wang GH, Ding F, Wang JL, Shen WF (2001) Phys Lett A280:325
11. Pithawalla YB, Deevi SC, El-Shall MS (2002) Mater Sci Eng A92:329–331
12. Becke AD (1993) J Chem Phys 98:1372
13. Lee C, Yang W, Parr RG (1988) Phys Rev B27:785
14. Handy NC, Schaefer III HF (1984) J Chem Phys 81:5031
15. Wadt WR, Hay PJ (1985) J Chem Phys 82:284
16. Nicklass A, Dolg M, Stoll H, Preuss H (1995) J Chem Phys 102:8942
17. Han JG (2003) Chem Phys 286:181
18. Han JG, Pang WM, Shi YY (2001) Chem Phys 263:255
19. Gaussian 98, Revision A9, Frisch MJ, Trucks GW, Schlegel HB, Scuseria GE, Robb MA, Cheeseman JR, Zakrzewski VG, Montgomery JA, Jr, Stratmann RE, Burant JC, Dapprich S, Millam JM, Daniels AD, Kudin KN, Strain MC, Farkas O, Tomasi J, Barone V, Cossi M, Cammi R, Mennucci B, Pomelli C, Adamo C, Clifford S, Ochterski J, Petersson GA, Ayala PY, Cui Q, Morokuma K, Malick DK, Rabuck AD, Raghavachari K, Foresman JB, Cioslowski J, Ortiz JV, Baboul AG, Stefanov BB, Liu G, Liashenko A, Piskorz P, Komaromi I, Gomperts R, Martin RL, Fox DJ, Keith T, Al-Laham MA, Peng CY, Nanayakkara A, Challacombe M, Gill PMW, Johnson B, Chen W, Wong MW, Andres JL, Gonzalez C, Head-Gordon M, Replogle ES, Pople JA (1998) Gaussian, Inc, Pittsburgh
20. Purdum H, Montano PA, Shenoy GK, Morrison T (1982) Phys Rev B25:4412
21. Montano PA, Shenoy GK (1980) Solid State Commun 35:53
22. Moskovits M, Dilella DP, Limm W (1984) J Chem Phys 80:626
23. Moskovits M, Dilella DP (1980) J Chem Phys 73:4917
24. Harris J, Jones RO (1979) J Chem Phys 70:830
25. Pulay P (1969) Mol Phys 17:197; (1979) Theor Chim Acta 50:299
26. Shim I, Gingerich KA (1982) J Chem Phys 77:2490
27. Dhar S, Kestdner NR (1988) Phys Rev A38:1111
28. Huber KP, Herzberg G (1979) Molecular spectra & molecular structure, constants of diatomic molecules. Van Nostrand-Reinhold, New York
29. Castro M, Salahub DR (1994) Phys Rev B49:11842
30. Majumder C, Kulsheshtha SK (2000) Chem Phys Lett 323:393
31. Veno J, Hoshino T, Hata M, Tsuda M (2000) App Surf Sci 440:162–163
32. Jones RO (1993) J Chem Phys 99:1194
33. Meier U, Peyerimhoff SD, Grein F (1990) Z Phys D17:209
34. Pacchioni G, Koutecky J, Bunsenges Ber (1984) Phys Chem 88:242; Koutecky J, Pacchioni G, Jeung GH, Hass EC (1985) Surf Sci 156:650
35. Petterson LGM, Bauschicher CW Jr, Halicioglu T (1987) J Chem Phys 87:2205
36. Desai PD (1987) J Phys Chem Ref Data 16:109